HAL
open science

Nuclear spin-spin interactions in CdTe probed by zero and ultra-low-field optically detected NMR

V. M. Litvyak, P. Bazhin, Régis André, Masha Vladimirova, K. V. Kavokin

To cite this version:

V. M. Litvyak, P. Bazhin, Régis André, Masha Vladimirova, K. V. Kavokin. Nuclear spin-spin interactions in CdTe probed by zero and ultra-low-field optically detected NMR. 2024. hal-04525413

HAL Id: hal-04525413

https://hal.science/hal-04525413v1

Preprint submitted on 28 Mar 2024

HAL is a multi-disciplinary open access archive for the deposit and dissemination of scientific research documents, whether they are published or not. The documents may come from teaching and research institutions in France or abroad, or from public or private research centers.

L'archive ouverte pluridisciplinaire **HAL**, est destinée au dépôt et à la diffusion de documents scientifiques de niveau recherche, publiés ou non, émanant des établissements d'enseignement et de recherche français ou étrangers, des laboratoires publics ou privés.

Nuclear spin-spin interactions in CdTe probed by zero and ultra-low-field optically detected NMR.

V. M. Litvyak,[1] P. Bazhin,[1] R. André,[2] M. Vladimirova,[3] and K. V. Kavokin[1]

[1] *Spin Optics Laboratory, St. Petersburg State University, 198504 St. Petersburg, Russia*
[2] *Université Grenoble Alpes, CNRS, Institut Néel, 38000 Grenoble, France*
[3] *Laboratoire Charles Coulomb, UMR 5221 CNRS/Université de Montpellier, France*

(Dated: March 27, 2024)

Nuclear magnetic resonance (NMR) is particularly relevant for studies of internuclear spin coupling at zero and ultra-low fields (ZULF), where spin-spin interactions dominate over Zeeman ones. Here we report on ZULF NMR in CdTe. In this semiconductor all magnetic isotopes have spin $I = 1/2$, so that internuclear interactions are never overshadowed by quadrupole effects. Our experiments rely on warm-up spectroscopy, a technique that combines optical pumping, additional cooling via adiabatic demagnetisation, and detection of the oscillating magnetic field-induced warm-up of the nuclear spin system via Hanle effect. We show that NMR spectra exhibit a rich fine structure, consistent with the low abundance of magnetic isotopes in CdTe, their zero quadrupole moments, as well as direct and indirect interactions between them. A model assuming that the electromagnetic radiation is absorbed by nuclear spin clusters composed of up to 5 magnetic isotopes allows us to reproduce the shape of a major part of the measured spectra.

arXiv:2403.17593v1 [cond-mat.mes-hall] 26 Mar 2024

I. INTRODUCTION

Nuclear spin interactions provide a wealth of information about the connectivity and spatial ordering of atoms in solid materials [1], they determine thermodynamics of the nuclear spin system [2] and are of crucial importance in many domains, spreading from physics, chemistry and biology [3] to quantum information processing [4]. Experimentally these interactions are probed via nuclear magnetic resonance (NMR) experiments, where absorption of the electromagnetic radiation as a function of its frequency is measured at relatively high static magnetic field.

In semiconductors, nuclei with non-zero magnetic moments participate in direct dipole-dipole and indirect (exchange and pseudodipolar) interactions [5]. The strength of these internuclear interactions is deduced from the shape of NMR lines at high external magnetic fields, where nuclear Zeeman energies are many orders of magnitude higher than the spin-spin ones.

The magnetic dipole-dipole interaction is the most long-range type of internuclear spin-spin interactions. Even at high magnetic field it is non-trivial to determine theoretically the precise shape of the absorption spectrum due to dipole-dipole coupling, but its contribution to the widths of NMR lines was calculated by Van Vleck in 1948 [6].

Indirect interactions (exchange and pseudodipolar) were included into consideration somewhat later. These interactions are mediated by valence electrons, and differ from zero only for the nearest neighbor nuclei. For example, the indirect exchange interaction was experimentally detected from the broadening of NMR lines in GaSb [7] and in GaAs [8]. The theoretical description was provided in [9]. The pseudodipolar interaction was first mentioned in Ref. 10. Then it was found that the pseudodipolar interaction in GaAs crystals cancels a considerable part of the dipole-dipole contribution to the second moment of NMR lines [11, 12]. The values of the isotope parameters and interaction constants in GaAs are reported in Tables I,II. Here D characterises direct dipole-dipole coupling between nearest neighbors, $J_\perp$ and $J_\parallel$ account for the anisotropy of the exchange interaction between two neighboring nuclei with respect to the axis of the interatomic bonds, see Sec. III.

Because in traditional high-field NMR spin-spin interaction energies are many orders of magnitude smaller than Zeeman ones, the only terms of the spin-coupling Hamiltonians that may be observed in such experiments are those that commute with the Zeeman Hamiltonian. Furthermore, spin-spin interactions usually make more subtle contributions to the zero-field NMR spectrum than quadrupole interactions. Therefore spin-spin interactions can be difficult to determine in the systems with spins greater than 1/2 if any non-intentional residual electric field gradients are present [12, 13]. However, because NMR sensitivity depends on magnetization magnitude and precession frequency, and both decrease when the magnetic field is decreased, measurements of the spin-spin interactions at low fields are particularly challenging.

Starting with the pioneering works in 1980s [14, 15], a trend has developed toward optically detected NMR (ODNMR) using submicrotesla fields or even no external field at all. In semiconductors, where deep cooling of the nuclear spin system can be reached by optical pumping followed by adiabatic demagnetisation to zero field, a specific approach to zero and ultra-low field (ZULF) NMR, termed as warm-up spectroscopy, has been proposed in Ref. [15]. The warm-up spectroscopy has been further developed in [13]. The method is based on the measurements of the oscillating magnetic field (OMF)-induced modifications of the nuclear spin temperature. This concept is particularly relevant in

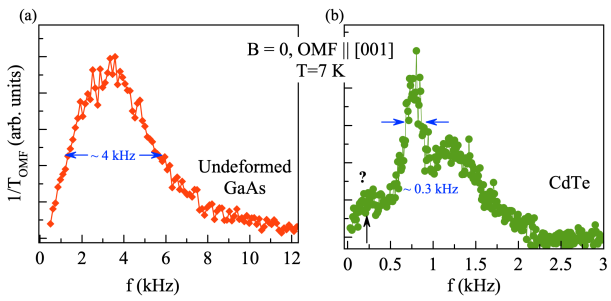

Figure 1. Absorption spectra of optically cooled NSS in zero magnetic field in bulk n-GaAs, see Ref. 12 (a) and in wide CdTe quantum well studied in this work (b).

ZULF regime, where it has been successfully employed for the description of a plethora of the experimental data [12, 13, 16, 17]. However, only few ZULF ODNMR experiments in semiconductors are currently available, and they mainly address GaAs based samples [12, 13, 18, 19].

The absorption spectrum of the lightly n-doped GaAs crystal measured in Ref. 12 by warm-up technique at zero magnetic field is shown in Fig. 1 (a). It presents a single broad peak at the frequency $f \approx 3.5$ kHz, with full width at half maximum (FWHM) ≈ 4 kHz. Unfortunately, theoretical calculation of such a spectrum in ZULF regime and thus identification of different kinds of the spin-spin interactions on the basis of comparison with the data is prohibitively complex, due to long-range nature of the dipole-dipole coupling and potentially nonzero quadrupole contribution.

In this context, CdTe is a very promising material. It has a zinc-blend crystal structure, similar to GaAs, but its nuclear spin system (NSS) is very dilute, only about one-third of the nuclei have a non-zero magnetic moment. The direct dipole-dipole coupling is rather weak, as compared to GaAs, where all the isotopes are magnetic [6]. On the other hand, high atomic numbers favor stronger indirect spin-spin coupling, see Table II. Finally, in contrast with GaAs, all magnetic isotopes have spin $I = 1/2$, so that quadrupole effects can not mask internuclear coupling. The main characteristics of CdTe isotopes with nonzero magnetic moments, as well as known from the literature parameters characterizing their interactions are summarized in Tables I, II [20]. For comparison, the same parameters for GaAs are reported.

The peculiarities of nuclear spin-spin interactions in CdTe crystals were discovered by Nolle and co-workers using traditional high-field NMR spectroscopy (B = 2.114 T) [21–23]. These measurements required significant acquisition times, about 12 h/spectrum, and provided remarkable results. Spectra around resonance frequency of ^{125}Te for different orientations of the crystal with respect to the external magnetic field appeared to have complex structure consisting of the main line

	I	γ (kHz/G)	A_{hf} (μeV)	A	P_m
^{69}Ga	3/2	1.03	43.1	0.6	1.0
^{71}Ga	3/2	1.29	54.8	0.4	1.0
^{75}As	3/2	0.73	43.5	1.0	1.0
GaAs	3/2	0.93	91	2.0	
^{111}Cd	1/2	-0.91	-37.4	0.13	0.91
^{113}Cd	1/2	-0.95	-39.1	0.12	0.91
^{125}Te	1/2	-1.35	-45	0.08	0.75
^{123}Te	1/2	-1.12	-45	0.01	0.75
CdTe	1/2	-0.17	-13	0.34	

Table I. Magnetic isotope parameters. Gyromagnetic ratio γ, hyperfine constant A_{hf}, abundance A, and the probability to have a magnetic neighbor P_m. Average values of γ and A_{hf}, as well as the total abundances of magnetic isotopes per unit cell consisting of two atoms in CdTe and in GaAs are given[24]. We neglect in this work ^{123}Te, a magnetic isotope with very low abundance.

	$J_\perp$ (kHz)	$J_\parallel$ (kHz)	D (kHz)
^{69}Ga/^{75}As	0.034^a, -0.339^b	0.643^a, 0.678^b	0.339
^{71}Ga/^{75}As	0.043^a, -0.43^b	0.817^a, 0.86^b	0.43
^{111}Cd/^{125}Te	0.723	0.42	0.364
^{111}Cd/^{125}Te	0.765	0.435	0.38

Table II. Spin-spin coupling constants from Ref. 22 in CdTe and from $[25]^a$, $[12]^b$ in GaAs.

and several satellites, depending on the field orientation. These fine structure was interpreted as being due to spin-spin interactions. The widths of the individual lines appeared to be as small as ≈ 0.2 kHz, roughly 10 times smaller than in GaAs crystals. This points out the significance of the difference between CdTe and GaAs NSS properties. From the measured spectra of ^{125}Te Nolle calculated the constants of pseudodipolar and exchange interactions reported in Table II, but, to the best of our knowledge, no experimental studies of the nuclear spin coupling at zero and low magnetic fields has been reported yet.

In this work we report on ZULF ODNMR experiments in CdTe. Fig. 1 (b) shows the absorption spectrum measured at zero magnetic field. As for GaAs (Fig. 1 (a)), the experiments are performed using warm-up spectroscopy [13], but in CdTe we observe multiple absorption lines, with much smaller FWHM, ≈ 0.3 kHz, consistent with dipole-dipole interaction between nearest neighbors.

In the absence of quadrupole interactions, the observed fine structure must be related to the internuclear spin coupling. We propose a model based on the hypothesis that NSS comprises mainly isolated noninteracting spins and small clusters consisting of up to 5 magnetic isotopes. The long-range interaction between clusters is neglected. Under these assumptions one can

reduce the problem of the interactions among all nuclei to the problem of the ensemble of interactions among a small number of nearest neighbors inside so-called nuclear spin clusters.

Using the hypothesis presented above, we calculate the spectral dependence of the NSS warm-up rate induced by the OMF at zero and low static magnetic fields for different orientations of the OMF with respect to the static field and the crystal axes, and compare these calculations with the experimentally measured spectra. An agreement between the model and the data is achieved in the absence of fitting parameters in most of the studied experimental configurations, suggesting the relevance and validity of the cluster model.

Most of the observed spectral features could be identified within the model on the basis of the internuclear interactions constants deduced from high-field NMR, except from the lowest frequency peak, indicated in Fig. 1 (b) by the arrow and the question mark. Its origin still needs to be clarified, but it could be related to some specific manifestations of the internuclear coupling in crystals, not observable in traditional NMR, because under high magnetic field these interactions are truncated by the Zeeman effect. Another discrepancy between the data and the model concerns the zero-field spectrum obtained in the configuration where OMF is oriented perpendicular to the sample surface. This could result from the incomplete thermalization within CdTe NSS.

The paper is organised as follows. In the next section we present the structure of the studied sample and the main principles of the the warm-up spectroscopy. More information about experimental protocol can be found in Appendix. The cluster model that we develop to calculate the warm-up spectra is introduced in Sec. III. In Section IV the experimentally measured spectra are presented and compared to the model predictions. Section V summarizes the results and points out some still unresolved issues.

II. SAMPLE AND EXPERIMENTAL TECHNIQUE

We study a 30-nm-wide CdTe quantum well (QW) sandwiched between $Cd_{0.95}Zn_{0.05}Te$ barriers. The top (bottom) barrier is 93(1064)-nm-thick. The sample is grown by molecular beam epitaxy on a [100] $Cd_{0.96}Zn_{0.04}Te$ substrate. Nuclear spin dynamics in this structure has been studied in Ref. [26]. An optical study of a very similar QW can be found in Ref. [27]. These studies confirm high quality of this type of structures and negligibly small exciton localization energy.

Though the sample is nominally undoped, low-temperature photoluminescence (PL) measurements reported in Ref. [26] indicate some unintentional doping. In wide CdTe/CdZnTe QWs excitonic states are known to be quantized as a whole, and in the studied structure the first excited state of the free exciton emits light at 1.602 eV [28]. This resonance is chosen to monitor PL polarization state in the detection part of the warm-up spectroscopy protocol described below. Importantly, although we study the NSS in the quantum layer in a heterostructure, the experiments presented here do not call on the QW-specific properties. Therefore, the NMR spectra reported below should be relevant for bulk CdTe crystals.

The experimental method that we implement to measure NMR spectrum is an all-optical technique, termed warm-up spectroscopy. It has been applied previously in GaAs[12, 13]. A typical measurement (see also Fig. 7 and Section VII) consists of five steps :

(i) Complete depolarization of the NSS by irradiation with OMF at f = 3 kHz during 10 s in zero static field and "in the dark".

(ii) Optical cooling of the NSS during 700 s in the presence of the longitudinal magnetic field B_p = 150 G (Faraday geometry). The excitation laser emits at 1.82 eV (far above QW barriers) and delivers 15 mW. It is circularly polarized and focused on a 100 μm-diameter spot on the sample surface.

(iii) Adiabatic demagnetisation "in the dark" from B_p to zero magnetic field within 20 ms, which results in additional cooling of the NSS [16, 17].

(iv) Application of the OMF B_{OMF} = 1 G at frequency f during t_{OMF} = 1 s. OMF field is applied either along the growth axis, or in the sample plane, either in presence or in absence of the static magnetic field B. Application of the OMF warms the NSS, the efficiency of this process depends on the difference between the OMF frequency f and the frequency of nuclear spin resonances.

(v) The last step consists in the measurement and quantitative analysis of the observed increase of the NSS temperature. To do so we switch on the transverse magnetic field B_m = 1.2 G (Voigt geometry) and the optical pumping. If the NSS is still cold enough, then an effective field $B_N(f)$ acting on the electrons resident in the QW will be created via hyperfine interaction. The magnitude of this field can be extracted from the PL polarisation degree as described in Appendix VII. The ratio between $B_N(f)$ and the nuclear field B_{N0} that we determine from the strictly identical experiment but without OMF, allows us to determine the OMF absorption rate at a given frequency as:

$$\frac{1}{T_{\mathrm{OMF}}}(f) = \frac{1}{t_{\mathrm{OMF}}}\ln\left(\frac{\mathrm{B_N(f)}}{\mathrm{B_{N0}}}\right). \quad (1)$$

By repeating the entire protocol for frequencies ranging from 30 Hz to 22 kHz we obtain the NMR spectrum at a given static field and orientation of the OMF. The detailed description of the procedure that allows as to determine $B_N(f)$ and B_{N0} is given in Appendix VII. All the measurements presented throughout this work are conducted at at T = 7 K.

An example of the NMR spectrum measured at B = 0 and OMF ∥ [001] is shown in Fig. 1 (b). The interpretation of this spectrum within the cluster model, as well

as the measurements in the presence of static fields and OMF with different orientations are reported in Sec. IV.

III. ABSORPTION OF THE ELECTROMAGNETIC RADIATION BY THE NSS: THE CLUSTER MODEL

In this section we develop a model that allows us to calculate the absorption of the electromagnetic radiation by the NSS in ZULF regime under the hypothesis that this absorption is determined by nuclear clusters. We start by defining the cluster as the set of magnetic isotopes located in a given way relative to each other. The nearest neighbors of a nucleus included in a cluster are either nuclei from the same cluster or non-magnetic nuclei.

We rank the clusters by their size, because, as will be shown below, their abundance in the crystal drops quickly as their size increases. Moreover, the clusters containing the same number, N, of magnetic nuclei may differ in the location of their nuclei relative to each other and to the crystal axes. The absorption of the electromagnetic radiation depends on both cluster size and its configuration. Examples of the clusters of different sizes are sketched in Fig. 2. The number of possible cluster configurations, C_N, increases rapidly with N, see Table III [29]. For example, a cluster containing two nuclei ($N = 2$) can be formed in four different ways, because every nucleus in the zinc-blend lattice of CdTe has four nearest neighbors. If one takes into account two magnetic isotopes of Cd, then the number of the configurations doubles, $C_N = 8$.

In general, for the cluster with N nuclei its appearance probability (or, equivalently, abundance), is given by the sum of the appearance probabilities over all possible configurations:

$$P_N = \sum_{l=1}^{C_N} P_{Nc}(l), \tag{2}$$

where the appearance probability of the l-th cluster with N magnetic isotopes, $P_{Nc}(l)$, is given by

$$P_{Nc}(l) = \frac{1}{N}\prod_{i=1}^{N} A(i)\cdot(1-P_m(i))^{4-G_N(i)}. \tag{3}$$

Here i is the index that goes over all magnetic isotopes in the l-th cluster, $A(i)$ is the abundance of the i-th isotope, $P_m(i)$ is the probability of the i-th isotope to have a magnetic nearest neighbor (see Table I), and $G_N(i)$ is the number of magnetic nearest neighbors of the i-th isotope in the l-th configuration.

Table III summarizes the probabilities calculated from Eqs. 2-3. One can see that the abundance of the clusters decreases rapidly as the cluster size increases. In the following we assume that only isolated single nuclei and the clusters with up to $N = 5$ nuclei contribute

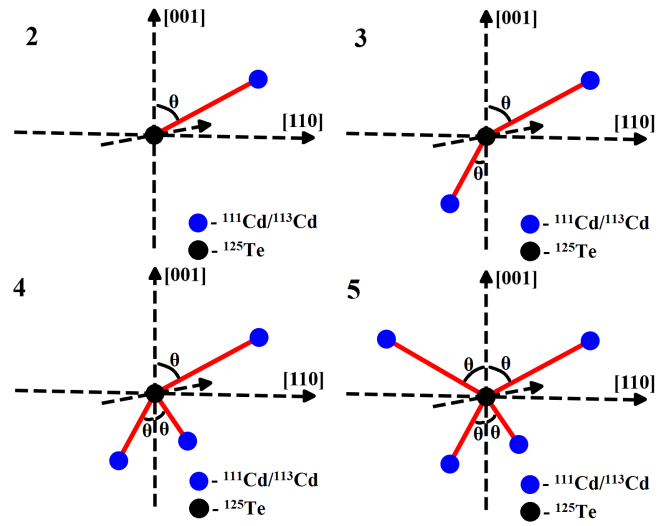

Figure 2. Sketch of the most frequent nuclear magnetic clusters in CdTe, with $N = 2$ to $N = 5$ spins. Blue circles are Cd isotopes, black circles are ^{125}Te, red lines indicate interatomic bonds, θ is the angle between interatomic bond and crystallographic axis.

to the absorption spectrum, and neglect larger clusters. We also suppose that different clusters do not interact between each other.

N	C_N	P_N
2	8	0.012
3	48	0.004
4	344	0.0013
5	2544	0.0006

Table III. Number of possible configurations and the appearance probability for the clusters with different size. Only clusters with ^{125}Te in the center are considered.

Under above assumptions, the absorption of radiation by the clusters of the size N is calculated as follows. First, for each configuration l from the total of C_N cluster's configurations, a Hamiltonian accounting for Zeeman interaction, as well as for direct and indirect spin-spin interactions can be written as:

$$\hat{H}_N(l) = h\Big[\sum_{i=1}^{N}\gamma^i(\vec{\hat{I}}^i\vec{B}) + \sum_{i<j}^{N}\delta^{ij}\sum_{k,s=x,y,z}\left(J^{ij}_{ks}+D^{ij}_{ks}\right)\hat{I}^i_k\hat{I}^j_s\Big]. \tag{4}$$

Here i is the index that goes over all nuclei in the cluster, h is the Planck constant, γ^i and $\vec{\hat{I}}^i$ are the gyromagnetic ratio and the spin operator of the i-th nuclei, respectively, $\vec{B}$ is the static magnetic field. $\delta^{ij} = 1$ if i-th and j-th nuclei are nearest neighbors, and zero otherwise. J^{ij} and D^{ij} are the tensors of indirect and direct

internuclear interactions, respectively. In the coordinate system defined by the principal axes, these tensors read:

$$J^{ij} = \begin{bmatrix} J_\perp & 0 & 0 \\ 0 & J_\perp & 0 \\ 0 & 0 & J_\parallel \end{bmatrix}; \; D^{ij} = \begin{bmatrix} D & 0 & 0 \\ 0 & D & 0 \\ 0 & 0 & -2D \end{bmatrix}, \tag{5}$$

where $J_\parallel$ and $J_\perp$ are the constants of indirect interaction between i-th and j-th nearest neighbor nuclei along the direction of the interatomic bond and perpendicular to it, respectively. Their values, reported by Nolle [22], are given in Table II. The direct interaction constant D is given by

$$D = \frac{\mu_0 \hbar}{4\pi} \frac{\gamma^i \gamma^j}{r_0^3}. \tag{6}$$

It characterises direct dipole-dipole interaction between i-th and j-th nearest neighbor nuclei, see Table II. Here μ_0 is the vacuum magnetic permeability, r_0 is the distance between nearest neighbors, $r_0 = 0.28$ nm in CdTe.

Tensors J^{ij} and D^{ij} are written in the coordinate system defined by the principal axis. It is directed along the internuclear bound, which is rotated by the angle θ with respect to the [001] crystallographic axis, see Fig. 2. Since in our experiments static and OMF fields are applied along the crystallographic axes we rotate these tensors by an angle θ for further calculations.

The Hamiltonians $\hat{H}_N(l)$ for each cluster configuration are diagonalised numerically yieldings an energy spectrum and a set of the corresponding wavefunctions. The OMF induces transitions between a pair of the cluster spin states if its frequency matches the energy difference between the energy levels. The probability of transition P_{mn} between energy levels E_m and E_n is given by $P_{mn} \propto M_{mn}^2$, where $M_{mn} = \langle \Psi_m | H_{\mathrm{OMF}} | \Psi_n \rangle$ is the matrix element of the Hamiltonian describing Zeeman interaction between $\vec{B}_{\mathrm{OMF}}$ and the nuclear spins:

$$H_{OMF} = h \sum_{i=1}^{N} \gamma^i \left(\vec{\hat{I}}^i \vec{B}_{\mathrm{OMF}} \right). \tag{7}$$

The warm-up rate associated with a given transition is proportional to its probability and to the square of its energy

$$\left. \frac{1}{T_{\mathrm{OMF}}} \right|_{mn} \sim P_{mn} |E_m - E_n|^2. \tag{8}$$

Assuming that the NSS is fully thermalized, the warm-up rate corresponding to the l-th configuration of the cluster containing N nuclei $\left.\frac{1}{T_{\mathrm{OMF}}}\right|_l$ is then obtained by the summation of the warm-up rates over all different pairs of states (m,n) within the cluster. Finally, the warm-up rate of the ensemble of the clusters containing

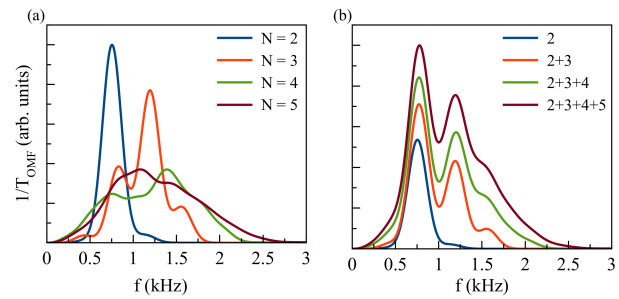

Figure 3. Calculated absorption of the OMF energy by the nuclear spin clusters in CdTe in zero magnetic field: (a) Absorption due to the clusters of a given size, from $N = 2$ to $N = 5$; (b) Absorption accounting for various combinations of the cluster sizes.

N nuclei is calculated as a sum over all possible configurations, taking into account their abundance:

$$\left. \frac{1}{T_{\mathrm{OMF}}} \right|_N = \sum_{l=1}^{C_N} P_{Nc}(l) \left. \frac{1}{T_{\mathrm{OMF}}} \right|_l. \tag{9}$$

The obtained rates are transformed into spectra by convoluting them with the Gaussians with FWHM= 0.3 kHz. A linewidth of this order of magnitude can be expected due to direct dipole-dipole interactions of the cluster nuclei with other magnetic nuclei in the crystal. Since the clusters of different sizes can contribute to the total absorption of the nuclear spin system, we also calculate spectra including combinations of clusters of different sizes. The resulting zero-field warm-up spectra for CdTe NSS are shown in Fig. 3. Individual contributions of the nuclear spin clusters of size N are shown in (a), while the combined absorption of the clusters with different sizes is shown in (b).

One can see that with increasing number of nuclei in the cluster the number of peaks in the spectrum grows up, the separation between them decreases, and the whole spectrum shifts towards higher energies. None of the spectra corresponding to the clusters of a given size matches the salient features of the measured spectrum shown in Fig. 1 (b), namely three distinct peaks and a high-frequency tail, but a combined contribution of all the clusters up to $N = 5$ does present a similar structure.

In the next Section we present nuclear spin absorption spectra measured for two different orientations of the OMF, in zero and low magnetic fields, and compare the data with the calculations performed within the cluster model.

IV. EXPERIMENTAL RESULTS AND COMPARISON WITH THE MODEL

Fig. 4 shows the OMF absorption spectra measured in zero static field for two different orientations of the

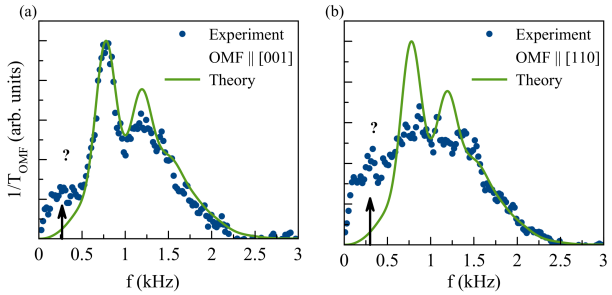

Figure 4. Zero-field absorption spectra measured (symbols) and calculated within the cluster model assuming the contribution of all the clusters containing up to five nuclei (lines). Twe different orientation of the OMF are explored, $B_{\mathrm{OMF}} \parallel [001]$ (a) and $B_{\mathrm{OMF}} \parallel [110]$ (b).

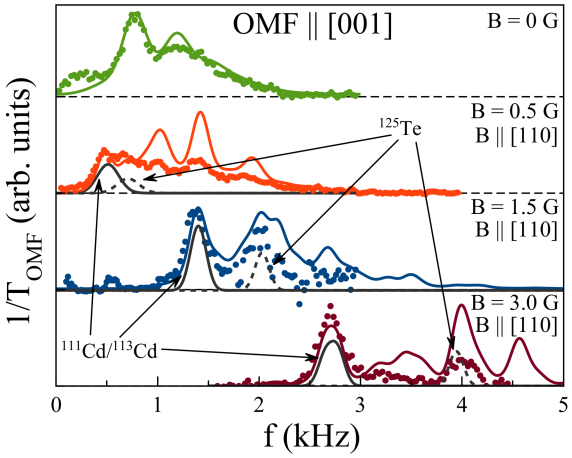

Figure 5. Absorption spectra measured under in-plane static field ($B \parallel [110]$) up to 3 G (symbols). Solid lines with the corresponding color code are the spectra calculated within cluster model and accounting for clusters up to $N = 5$. Solid and dashed gray lines represent absorption that one would expect from Zeeman splitting of individual, non-interacting Cd and Te isotopes, respectively.

OMF, either parallel (a), or perpendicular (b) to the growth axis. The spectrum in (a) is identical to the one shown in Fig. 1 (b), but here the spectra are compared to the calculation (lines) within the cluster model accounting for all the clusters up to $N = 5$ (see also green line in Fig. 3 (b)). One can see that the calculated spectrum matches relatively well the experimental one when the OMF is oriented along the growth axis (Fig. 4 (a)), except the lowest frequency peak at ≈ 0.25 kHz. This peak is indicated by the arrow and the question sign. It may be related to the dipole-dipole coupling between the same isotopic species separated by large distances, because this coupling is assumed to be weak, and is not included in the model. Estimations including up to 5 interacting Cd isotopes indicate that this contribution would no exceed one percent of the main absorption line spectral density. Thus, it may have another origin. We speculate that it could be related to some ZULF-specific manifestations of the internuclear coupling in crystals, which does not exist in traditional NMR, because under high magnetic field these interactions are truncated by the Zeeman effect.

Remarkably, in the case where the OMF is oriented in the QW plane (Fig. 4 (b)), the spectrum has a very different shape. While the integrated absorption is of the same order, the three-peaks fine structure is almost washed out, and only the higher-frequency tail persists. This result is quite surprising. Indeed, the rate of absorption at a given frequency is proportional to the imaginary part of magnetic susceptibility. The susceptibility is a second-rank tensor, which, in case of cubic symmetry, can only be a scalar. This symmetry conclusion is supported by numerical calculations within the cluster model, which gives exactly the same result for the two geometries. This significant discrepancy indicates that the model fails to describe a part of the NSS thermodynamics. We tentatively attribute this result to the incomplete thermalization within the NSS: spin clusters could retain memory of the direction in which they were initially polarized. Further research is required, however, to validate this hypothesis.

Evolution of the spectrum shown in Fig. 4 (a) upon increasing static magnetic field applied in the QW plane ($B \parallel [110]$) up to 3 G is shown in Fig. 5. One can see that the zero-field absorption peaks shift towards higher frequencies and additional peaks, corresponding to non-interacting ^{111}Cd, ^{113}Cd and ^{125}Te isotope's Zeeman splittings, start to form, *cf* black spectra calculated for such non-interacting nuclei. These Zeeman contributions to the spectra are also indicated by grey arrows. Note that at such low fields, the contributions of ^{111}Cd and ^{113}Cd are still not resolved, since they have very similar gyromagnetic ratios, see Teble I. The model reproduces faithfully the position of main absorption peaks but seems to overestimate the intensity of the blue side of the spectrum. As in the case of the [110]-oriented OMF absorption shown in Fig. 4 (b), this could suggest an incomplete thermalization within the NSS.

At higher magnetic fields, when Zeeman splittings of all isotopes significantly exceed internuclear interactions, a spectral structure similar to that measured by Nolle [22] is expected to be observed. At 2.114 T, Nolle observed Zeeman lines surrounded by the satellites, that he identified as being due to nuclear spin-spin interactions. The position of the satellite peaks has been shown to depend on the orientation of the static magnetic field. This experimental fact is a fingerprint of non-scalar pseudodipolar interactions. To check the validity of this argument in our sample, it is instructive to measure magnetic field orientation-dependent nuclear spin absorption in the regime where Zeeman interaction dominates over spin-spin coupling.

Such spectra are measured at $B \approx 15$ G for two per-

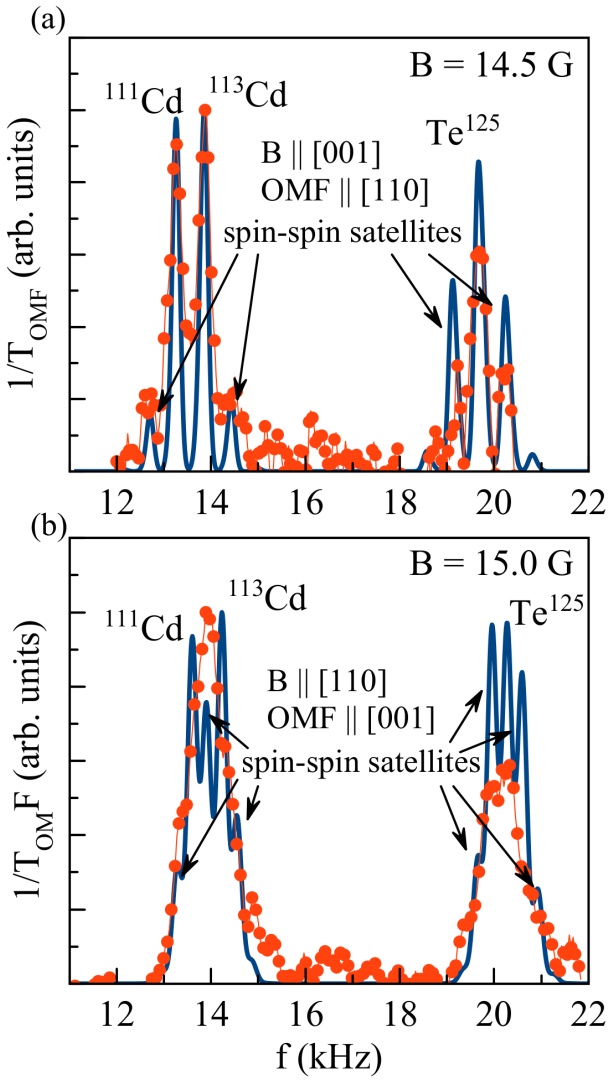

Figure 6. Measured (symbols) and calculated (lines) absorption spectra at static magnetic fields $B \approx 15$ G for two mutually orthogonal orientations of the oscillating and static magnetic field: (a) $B = 14.5$ G and || [110], OMF || [001]; (b) $B = 15$ G and || [001], OMF || [110].

pendicular orientations of the static field, see Fig. 6. For each of these measurements the OMF orientation was adjusted to be perpendicular to the static field. One can see that both spectra clearly demonstrate spin-spin satellites accompanying Zeeman absorption peaks. As in Ref. 22, the position of the satellites depends on the orientation of the magnetic field. This is correctly reproduced by the cluster model with N limited by 5 nuclei, and thus confirms its validity. We note, however, that similarly to lower-field data (Fig. 5), the intensity of the high-frequency peaks corresponding to ^{125}Te and its satellites is slightly overestimated as compared to the Cd-related low frequency part of the spectrum, and as in zero-field experiment (Fig. 4) (b)) the fine structure is somehow washed out in the OMF|| [100] geometry.

Finally, the signal associated with the very low abundance ^{123}Te isotope has not been identified in the measured spectra, justifying our choice to neglect it the calculations.

V. CONCLUSIONS

We have studied, experimentally and theoretically, the absorption of electromagnetic radiation by nuclear spins in wide CdTe/CdZnTe QW at zero and low magnetic fields. The reported results are not specific to heterostructures, and should apply as well to bulk CdTe crystals.

The absorption spectra are measured using warm-up spectroscopy, a multistage technique that comprises NSS preparation by optical pumping followed by adiabatic demagnetization, application of the OMF which heats the NSS at a given value of the static magnetic field, and measurement of the frequency-dependent NSS warm-up rate optically, via Hanle effect [13].

We found that CdTe NSS is characterized by much narrower absorption lines than GaAs NSS, which we have studied previously [12]. The main characteristics of the spectra, namely, the fine structure observed in zero magnetic field, as well as the satellite lines that emerge under magnetic field around the Zeeman lines of the three main magnetic isotopes, are understood in terms of internuclear coupling, on the basis of the "cluster model", that we developed for this purpose.

The model is based on the hypothesis that NSS in CdTe comprises mainly isolated noninteracting spins and small clusters consisting of up to 5 magnetic isotopes. It accounts for direct and indirect (exchange and pseudodipolar) interactions within the clusters, while the long-range interaction between the clusters is neglected. This allows us to simplify a prohibitively complex problem resulting from the long-range character of the dipolar interaction, and reduce it to a tractable one, in order to calculate the shape of the NSS absorption spectra.

The proposed model faithfully reproduces the position of the absorption peaks in most of the studied configurations (different values of the static field, its orientation with respect to the crystal axes), while it does not have any free parameters. The main experimentally observed features that still need to be understood include the lowest frequency peak at zero magnetic field spectrum, the overestimated intensity of the high-frequency part of the spectrum, as well as the unexpected difference between zero-field absorption spectra measured in OMF || [001] and OMF || [110] configurations. While the two later observations are probably related to the incomplete thermalization within the dilute NSS in CdTe, the former may point on the ZULF-specific manifestations of the internuclear coupling in crystals, that can

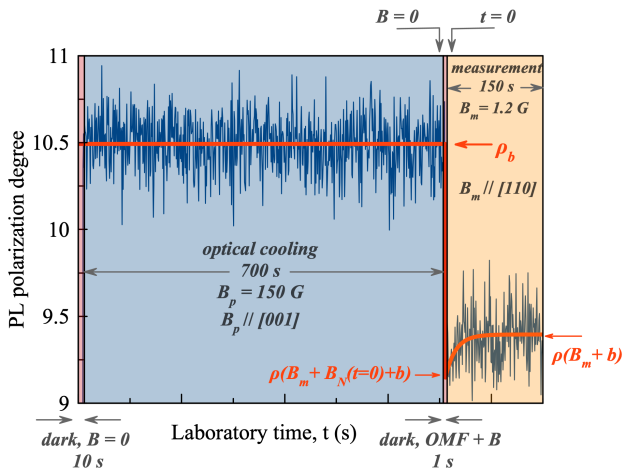

Figure 7. PL polarization degree measured (blue line) in a single warm-up experiment that allows for the determination of B_N at $t = 0$ by fitting (red line) Eqs. 10 and 11 to the data. Relevant values of the PL polarization are indicated by red arrows.

not be observed in traditional high-field NMR, where these interactions are negligibly small as compared to the Zeeman effect.

VI. ACKNOWLEDGEMENTS

The authors wish to thank Denis Scalbert and Boris Gribakin for inspiring discussions. Financial support from French National Research Agency, Grant No. ANR-21-CE30-0049 (CONUS) and from Russian Science Foundation, Grant No. 22-42-09020 is gratefully acknowledged. RA has benefited from the technical and scientific environment of the CEA-CNRS joint team "Nanophysics and Semiconductors".

VII. APPENDIX: MEASUREMENTS OF THE NSS WARM-UP RATE.

The five-stages experimental protocol described in Sec. II comprises the measurement stage, where nuclear field B_N [30], created by nuclei and acting on photocreated electrons, is extracted from the PL polarisation degree. We are interested in $B_N(t = 0)$, the value of B_N at $t = 0$, that is right after the application of the OMF. We denote this field as $B_N(f)$ when it builds up after the application of the OMF during t_{OMF}, and as B_{N0} in the reference experiment, were OMF is not applied. Once these fields are measured, the absorption rate at frequency f is readily obtained via Eq. 1.

To determine the field $B_N(t = 0)$, circularly polarized laser beam and the transverse measuring field B_{m} are switched on at $t = 0$, and then the PL polarization degree $\rho(t)$ is recorded during 150 s. The polarization recorded during the entire duration of the protocol, including the pumping stage, is illustrated in Fig. 7. Three important values of the PL polarization are indicated by red arrows. The polarization under optical pumping in the presence of the longitudinal field B_p is denoted as ρ_b, where the index indicates that it accounts for the presence of the field b, a small nuclear field brought about by nuclear spin cooling in the Knight field of photocreated electrons [13]. The polarization at $t = 0$ in the presence of both measurement field and the nuclear field is denoted as $\rho(B_m+B_N(t = 0)+b)$. The nuclear field $B_N(t = 0)$ is the one we need to extract from this measurement. Finally, the polarization $\rho(B_m + b)$ is reached at the end of the measurement stage, after complete depolarization of the NSS. One can see that ρ_b is higher than two other polarization values discussed above. This is the manifestation of the Hanle effect, that predicts depolarization of the PL in the presence of the transverse field and provides the relation between the value of the transverse field and PL polarization.

Assuming that during measurements nuclear spin polarization decays exponentially with a characteristic time T_1, the PL polarization degree in the total magnetic field experienced by electrons $B_{\mathrm{m}} + B_N(t) + b$ can be written as [31]:

$$\rho(t) = \rho_b \frac{B_{1/2}^2}{B_{1/2}^2+\tilde{B}^2}, \tag{10}$$

where

$$\tilde{B} = [B_N(t = 0) - b]\exp(-t/T_1) + B_m + b. \tag{11}$$

Here $B_{1/2}$ and T_1 are the independently measured half-width of the Hanle curve and the PL depolarization time, respectively.

Fitting Eq. 10 to the data like those shown in Fig. 7 allows us to determine $B_N(t = 0)$. In the case where the OMF at frequency f is applied prior to measurements, we have $B_N(t = 0) \equiv B_N(f)$, and in the reference experiment without OMF we have $B_N(t = 0) \equiv B_{N0}$. Finally, the absorption rate is obtained from the Eq. 1.

[1] A. Abragam, *The principles of nuclear magnetism* (Clarendon Press, 1961).
[2] M. Goldman, *Spin Temperature and Nuclear Magnetic Resonance in Solids* (Oxford University Press, 1970).
[3] W. Kemp, *NMR in Chemistry* (Macmillan Education UK, London, 1986).

[4] I. S. Oliveira, T. J. Bonagamba, R. S. Sarthour, J. C. C. Freitas, and E. R. deAzevedo, 5 - Implementation of Quantum Algorithms by NMR, in *NMR Quantum Information Processing*, edited by I. S. Oliveira, T. J. Bonagamba, R. S. Sarthour, J. C. C. Freitas, and E. R. deAzevedo (Elsevier Science B.V., Amsterdam, 2007) pp. 183–205.

[5] D. Paget, G. Lampel, B. Sapoval, and V. I. Safarov, Low field electron-nuclear spin coupling in gallium arsenide under optical pumping conditions, Phys. Rev. B **15**, 5780 (1977).

[6] J. H. Van Vleck, The Dipolar Broadening of Magnetic Resonance Lines in Crystals, Physical Review **74**, 1168 (1948), publisher: American Physical Society.

[7] R. G. Shulman, J. M. Mays, and D. W. McCall, Nuclear Magnetic Resonance in Semiconductors. I. Exchange Broadening in InSb and GaSb, Physical Review **100**, 692 (1955), publisher: American Physical Society.

[8] R. G. Shulman, B. J. Wyluda, and H. J. Hrostowski, Nuclear Magnetic Resonance in Semiconductors. III. Exchange Broadening in GaAs and InAs, Physical Review **109**, 808 (1958).

[9] P. W. Anderson and H. Hasegawa, Considerations on Double Exchange, Physical Review **100**, 675 (1955).

[10] N. Bloembergen and T. J. Rowland, Nuclear Spin Exchange in Solids: Tl^{203} and Tl^{205} Magnetic Resonance in Thallium and Thallic Oxide, Physical Review **97**, 1679 (1955).

[11] R. K. Hester, A. Sher, J. F. Soest, and G. Weisz, Nuclear-magnetic-resonance detection of charge defects in gallium arsenide, Physical Review B **10**, 4262 (1974).

[12] V. M. Litvyak, R. V. Cherbunin, V. K. Kalevich, and K. V. Kavokin, Local field of spin-spin interactions in the nuclear spin system of n-GaAs, Physical Review B **108**, 235204 (2023), publisher: American Physical Society.

[13] V. M. Litvyak, R. V. Cherbunin, V. K. Kalevich, A. I. Lihachev, A. V. Nashchekin, M. Vladimirova, and K. V. Kavokin, Warm-up spectroscopy of quadrupole-split nuclear spins in\textbackslashemph n-GaAs epitaxial layers, Physical Review B **104**, 235201 (2021).

[14] D. B. Zax, A. Bielecki, K. W. Zilm, and A. Pines, Heteronuclear zero-field NMR, Chemical Physics Letters **106**, 550 (1984).

[15] V. K. Kalevich and V. G. Fleisher, Optical detection of NMR with dynamic cooling of the nuclear spin system of a semiconductor by polarized light, Bull. Acad. Sci. USSR Phys. Ser. **47**, 5 (1983).

[16] A. Abragam and W. G. Proctor, Spin temperature, Phys. Rev. **109**, 1441 (1958).

[17] M. Vladimirova, S. Cronenberger, D. Scalbert, I. I. Ryzhov, V. S. Zapasskii, G. G. Kozlov, A. Lemaître, and K. V. Kavokin, Spin temperature concept verified by optical magnetometry of nuclear spins, Phys. Rev. B **97**, 041301 (2018).

[18] R. Giri, S. Cronenberger, M. M. Glazov, K. V. Kavokin, A. Lemaître, J. Bloch, M. Vladimirova, and D. Scalbert, Nondestructive Measurement of Nuclear Magnetization by Off-Resonant Faraday Rotation, Physical Review Letters **111**, 087603 (2013).

[19] M. Vladimirova, S. Cronenberger, A. Colombier, D. Scalbert, V. M. Litvyak, K. V. Kavokin, and A. Lemaître, Simultaneous measurements of nuclear-spin heat capacity, temperature, and relaxation in GaAs microstructures, Physical Review B **105**, 155305 (2022).

[20] We neglect in this work ^{123}Te, a magnetic isotope with very low abundance [24].

[21] W. Koch, O. Lutz, and A. Nolle, ^{77}Se and ^{125}Te nuclear magnetic resonance investigations in II–VI and IV–VI compounds, Zeitschrift für Physik A Atoms and Nuclei **289**, 17 (1978).

[22] A. Nolle, Direct and indirect dipole-dipole coupling between ^{111}Cd,^{113}Cd and ^{125}Te in solid CdTe, Zeitschrift für Physik B Condensed Matter **34**, 175 (1979).

[23] R. Balz, M. Haller, W. E. Hertler, O. Lutz, A. Nolle, and R. Schafitel, 125Te NMR studies of indirect and direct dipole-dipole coupling in polycrystalline CdTe, HgTe, and PbTe, Journal of Magnetic Resonance (1969) **40**, 9 (1980).

[24] R. K. Harris, E. D. Becker, S. M. Cabral De Menezes, R. Goodfellow, and P. Granger, NMR nomenclature: Nuclear spin properties and conventions for chemical shifts (IUPAC recommendations 2001), Concepts in Magnetic Resonance **14**, 326 (2002).

[25] M. K. Cueman and J. F. Soest, Pseudodipolar and exchange broadening of NMR lines in GaP and GaAs, Physical Review B **14**, 13 (1976).

[26] B. F. Gribakin, V. M. Litvyak, M. Kotur, R. André, M. Vladimirova, D. R. Yakovlev, and K. V. Kavokin, Nuclear spin relaxation mediated by donor-bound and free electrons in wide cdte quantum wells (2024), arXiv:2402.17435.

[27] A. V. Mikhailov, A. S. Kurdyubov, E. S. Khramtsov, I. V. Ignatiev, B. F. Gribakin, S. Cronenberger, D. Scalbert, M. R. Vladimirova, and R. André, Exciton dynamics in CdTe/CdZnTe quantum well (2023), arXiv:2304.07135.

[28] Y. M. d'Aubigné, H. Mariette, N. Magnea, H. Tuffigo, R. T. Cox, G. Lentz, L. S. Dang, J.-L. Pautrat, and A. Wasiela, Optical properties of CdTe/Cd_{1-x}Zn_xte quantum wells and superlattices, Surface Science **101**, 650 (1990).

[29] Only clusters with single ^{125}Te are considered in this work, since it has much lower abundance than magnetic isotopes of Cd.

[30] A. W. Overhauser, Polarization of nuclei in metals, Phys. Rev. **92**, 411 (1953).

[31] F. Meier and B. P. Zakharchenya, eds., *Optical Orientation* (North Holland, Amsterdam, 1984).